A complex Ar···Ag–I produced by laser ablation and characterised by rotational spectroscopy and *ab initio* calculations: Variation of properties along the series Ar···Ag–X (X= F, Cl, Br and I)

Chris Medcraft,[a] John C. Mullaney,[a] Nicholas R. Walker[a]* and Anthony C. Legon[b]*

[a]*School of Chemistry, Newcastle University, Bedson Building, Newcastle-upon-Tyne, NE1 7RU, UK*

[b]*School of Chemistry, University of Bristol, Cantock's Close, Bristol, BS8 1TS, UK.*

Abstract

A complex of argon with silver iodide (Ar···Ag−I) has been formed in the gas phase by laser ablation of a silver iodide rod in the presence of a pulse of argon gas and its ground-state rotational spectrum has been detected by means of a chirped-pulse, F-T microwave instrument. Ar···Ag−I was characterised both by experimental properties determined from its rotational spectrum and by *ab initio* calculations carried out at the CCSD(T)(F12c)/cc-pVTZ-F12 explicitly correlated level of theory. The molecule was shown to be linear in the ground state, with atoms in the order shown. The Ar···Ag and Ag–I bond lengths r_0(Ar···Ag) = 2.6759 Å and r_0(Ag–I) = 2.5356 Å, the dissociation energy D_e = 16.7 kJ mol^{-1} for the process Ar···Ag−I = Ar + Ag−I, the intermolecular quadratic stretching force constant $F_{\mathrm{Ar\cdots Ag}} = F_{22}$ = 20.2 N m^{-1} and the increase 0.033 in the ionicity i_c of Ag–I when it enters the complex are reported. The opportunity has been taken to compare the way in which these properties vary along the series Ar···Ag−X (X = F, Cl, Br and I).

**Email address:* a.c.legon@bristol.ac.uk, nick.walker@newcastle.ac.uk

1 Introduction

Complexes of argon with silver halides Ag–X (X = F, Cl and Br) were first identified and characterised in the gas phase by Evans and Gerry [1] by means of rotational spectroscopy. The silver halide was produced by allowing the plasma generated by laser ablation of metallic silver to react with a pulse of argon gas carrying a small concentration of halogen precursor (SF_6, Cl_2 or Br_2, respectively). The pulse of gas was then allowed to expand into the Fabry-Perot cavity of a Fourier-transform, microwave spectrometer of design similar to that described by Balle and Flygare [2]. Detailed analyses of the rotational spectra of the new species Ar···Ag-X established that they were linear molecules, with the atoms in the indicated order. Estimates of two measures of the binding strength revealed that the complexes Ar···Ag-X were rather more strongly bound than expected from experience with, for example, the corresponding hydrogen-bonded complexes Ar···H−X[3-6] or halogen-bonded complexes Ar···X−Y [7-10]. One measure of binding strength was the intermolecular stretching force constant, as obtained from the centrifugal distortion constant D_J by assuming Ag–X to be a point mass, while the other was the dissociation energy D_e for the process Ar···Ag–X = Ar + Ag–X, as obtained through *ab initio* calculation.

The final member of the series Ar ···Ag–X has X = I and was not investigated in ref. 1. Although we have established that trifluoroiodomethane, F_3C–I, serves as a convenient source of iodine when used in laser-ablation experiments of the type outlined in the preceding paragraph [11], we were unable to observe Ar ···Ag–I in this way. Instead, we detected this species when using a rod containing silver iodide. We report here the observation of the rotational spectra of the two isotopologues ^{40}Ar ···^{107}Ag–^{127}I and ^{40}Ar···^{109}Ag–^{127}I. Analyses of these spectra yields the rotational constant B_0, the centrifugal distortion constant D_J and the iodine nuclear quadrupole coupling constant χ_{aa}(I) for the ground state of each isotopologue. We take the opportunity presented by this new experimental work to discuss the variation of geometry, binding strength and electric charge rearrangement within Ag–X on formation of each member of the series Ar···Ag−F, Ar···Ag–Cl, Ar···Ag–Br and Ar···Ag–I in the light of two recent advances, namely (a) a two-force constant model which treats the Ag−X subunit as non-rigid and extended in space rather than as a point mass (*i.e.* the Ag–X quadratic stretching force constant is assumed finite), and (b) *ab initio* calculations at the explicitly correlated level CCSD(T)(F12c)/cc-pVTZ-F12,

which lead to improved estimates of equilibrium bond lengths r_e(Ar···Ag) and r_e(Ag–X) and equilibrium bond dissociation energies D_e for the process Ar···Ag–X = Ar + Ag–X.

2 Experimental and theoretical methods

2.1 Detection of the rotational spectrum.

A chirped-pulse Fourier-transform microwave (CP-FTMW) spectrometer fitted with a laser ablation source was used to observe the rotational spectra of Ar···Ag–I in the frequency range 6.5 to 18.5 GHz (see Figure 1). The spectrometer and laser ablation source have been described in detail elsewhere [12,13] A carrier gas consisting of argon held at a total pressure of 6 bar was pulsed over the surface of a rod containing silver iodide that was ablated by a suitably timed Nd:YAG laser pulse (wavelength 532 nm, pulse duration 10 ns, pulse energy 20 mJ). The gas pulse expanded supersonically into the vacuum chamber of the spectrometer. Translation and rotation of the rod at regular, short intervals ensured that each laser pulse (repetition rate of ~1.05 Hz) impinged on a fresh surface. This improves shot-to-shot reproducibility.

The sequence of steps employed to record broadband microwave spectra was as follows. First, polarisation of the sample was achieved by means of a microwave chirp that sweeps from 6.5 to 18.5 GHz within 1 μs. Secondly, the free induction decay (FID) of the molecular emission following the polarization was recorded over a time period of 20 μs. This sequence was repeated eight times during the period of the expansion of each gas pulse. The FID was mixed down with the signal from a 19 GHz local oscillator and then digitized by means of a 25 Gs/s digital oscilloscope. Each transition is observed as a single peak with full-width at half-maximum (FWHM) ≅ 100 kHz after application of a high-resolution window function. The estimated accuracy of frequency measurement was *ca.* 10 kHz.

2.2 Ab initio calculations

Structure optimizations were conducted for the series of Ar···Ag–X (X = F, Cl, Br and I) using the MOLPRO package [14] at the CCSD(T)(F12c) level of theory [15], a coupled-cluster method with single and double excitations, explicit correlation [16] and a perturbative treatment of triple excitations [17]. Counter-poise corrected dissociation energies were calculated using the Boys-Bernardi method [18]. When correcting the dissociation energies for basis set superposition

error (BSSE) using the version of MOLPRO available, it was necessary for numerical stability to exclude the CABS singles correction term [19,20] for Ar···Ag–Br and Ar···Ag–I. A basis set combination consisting of cc-pVTZ-F12 optimised functions on the Ar, F and Cl atoms and cc-pVTZ-PP-F12 optimised functions on the I and Br atoms [21] were used. For Ag, the corresponding cc-pVTZ-F12 optimised functions are not yet available. Instead, we used some auxiliary basis sets developed by Hill and Peterson [22] to allow aug-cc-pVTZ basis sets for Ag to be used in F12 calculations. The resolution-of-the-identity within the F12 methodology employed the aug-cc-pVTZ/OptRI complementary auxiliary basis set for Ag. ECP-10-MDF [23,24] was used on Br and ECP-28-MDF [25] on Ag and I, respectively, to account for scalar relativistic effects. Geometry optimisations were conducted and quadratic force constants were calculated for the isolated silver halides Ag–X (X=F, Cl, Br and I) at the same level of theory.

3 Results

3.1 Determination of spectroscopic constants

The rotational spectrum attributed to Ar···Ag–I showed evidence of the presence of the two almost equally-abundant isotopologues ^{40}Ar···^{107}Ag–^{127}I and ^{40}Ar··· ^{109}Ag–^{127}I. Each spectrum was characteristic of a closed-shell, linear molecule in its zero-point state and each exhibited iodine nuclear quadrupole hyperfine structure, as is evident by examination of the spectrum shown in Figure 1. An iterative least-squares fit of the observed hyperfine frequencies of several J+1→J transitions for each isotopologue was carried out by using the program PGOPHER, written and maintained by Western [26]. The Hamiltonian employed was of the form

$$H = H_R - \tfrac{1}{6}\mathbf{Q}:\boldsymbol{\nabla}\mathbf{E} \qquad (1),$$

where H_R is the usual rotational energy operator for a semi-rigid, linear molecule and $-\tfrac{1}{6}\mathbf{Q}:\boldsymbol{\nabla}\mathbf{E}$ is the iodine nuclear quadrupole energy operator, in which $\mathbf{Q}$ is the iodine nuclear electric quadrupole moment tensor and $\boldsymbol{\nabla}\mathbf{E}$ is the electric field gradient tensor at I. The H matrix was constructed in the coupled basis $\boldsymbol{I} + \boldsymbol{J} = \boldsymbol{F}$. The only spectroscopic constants necessary to fit all of the observed transitions of each isotopologue to within the estimated accuracy of frequency measurement (10 kHz) were the rotational constant B_0, the quartic centrifugal distortion constant D_J, and the iodine nuclear quadrupole coupling constant $\chi_{aa}(\mathrm{I}) = -eQ\,{}^{\partial^2 V}/_{\partial a^2} =$

eQq_{aa} (where $q_{aa} = {}^{-\partial^2 V}/_{\partial a^2}$ is the electric field gradient along the axis of the linear molecule). The effects of iodine spin-rotation coupling were too small to detect and the corresponding term was therefore not included in eq.(1). The sign and magnitude of the nuclear quadrupole coupling constant provides strong evidence that the molecule contains iodine; the identification of two Ag isotopologues likewise indicates the presence of silver; the evidence that the molecule contains argon is less direct and relies on the internal consistency of what follows in this article. The form of the observed spectrum is also consistent with a very slightly bent triatomic molecule, with a potential energy barrier to the linear conformation sufficiently low that the ground-state wavefunction has $C_{\infty v}$ symmetry but the results of the *ab initio* calculations referred to in Section 2.2 ruled out this possibility (see later).

Values of the spectroscopic constants from the final cycle of the PGOPHER fit are shown in Table 1 for the two isotopologues Ar··· ^{107}Ag–I and Ar··· ^{109}Ag–I investigated, together with σ_{RMS}, the RMS deviation of the fit, and *N*, the number of iodine hyperfine components fitted. The values of σ_{RMS} are satisfactory, given the estimated accuracy of frequency measurement (10 kHz) associated with the chirped-pulse F-T microwave spectrometer. The detailed fits are available as Supplementary Material. A spectrum simulated by using PGOPHER and the sets of spectroscopic constants reported in Table 1 is also included in Figure 1.

3.2 Molecular geometry

The observed ground-state rotational spectrum of the complex of Ar and Ag–I is consistent with a linear molecule in which the atoms are in the order Ar···Ag–I (see Figure 2). Isotopic substitution at the Ag atom allows the magnitude of the r_{s} coordinate [27,28] of that atom to be determined by means of the eq.(2).

$$\left|a_{\mathrm{Ag}}\right| = \{\Delta I_b/\mu_{\mathrm{s}}\}^{1/2} \qquad (2),$$

in which ΔI_b is the change in the moment of inertia on isotopic substitution and $\mu_{\mathrm{s}} = \Delta m M/(\Delta m + M)$ is the reduced mass for the substitution. The result is $\left|a_{\mathrm{Ag}}\right|$ =0.7852(12) Å, where the error is given by δa=0.0015/|*a*|, as recommended in ref.27. The Ag atom is sufficiently close to the centre of mass of the linear molecule that the only physically realistic order of the atoms is Ar···Ag–I.

Ab initio calculations at the CCSD(T)(F12c)/ccpVTZ-F12 level (described in Section 2.2) confirm that the molecule Ar···Ag–I is indeed linear in its equilibrium geometry with the angle ∠ArAgI =180° and therefore that only the two distances r(Ar···Ag) and r(Ag–I) are required to define its geometry. The equilibrium values r_e(Ar···Ag), r_e(Ag–I) and ∠ArAgI resulting from the *ab initio* calculation are recorded in the final column of Table 2. The availability of the rotational constants $B_0 = C_0$ for the two isotopologues ^{40}Ar··· ^{107}Ag–^{127}I and ^{40}Ar··· ^{109}Ag–^{127}I allows determination of r_0 versions of the two distances. When the ground-state moments of inertia of both isotopologues were fitted by means of Kisiel's program STRFIT [29], the results were r_0(Ar···Ag) = 2.6759 Å and r_0(Ag–I) = 2.5356 Å, which are also recorded in the final column of Table 2. No errors in these quantities are generated from the fit because two constants are fitted by two distances. It is of interest to note that the r_e and r_0 geometries of Ar···Ag–I given in Table 2 imply the values of 0.7898 and 0.7847 Å, respectively, for a_{Ag}, in good agreement with the substitution value 0.7852(12) Å.

3.3 Strength of the interaction of Ar and Ag–I

Although the interaction between Lewis bases B and coinage metal halides M–X (M = Cu, Ag or Au) in the molecules B–M–X can be sufficient to give B–M bonds of similar strength to the M–X bond [30,31], we begin here with the assumption that the Ag–I bond is much stronger than that of Ar···Ag. The strength of the Ar···Ag interaction can be then be described either by the intermolecular stretching quadratic force constant $F_{Ar\cdots Ag}$ or by the energy D_e required to dissociate the molecule according to Ar···Ag–I = Ar + Ag–I, all molecules in their hypothetical equilibrium configurations. $F_{Ar\cdots Ag}$ is the curvature at the minimum of the potential energy curve generated by plotting the energy of the system as a function of the distance r(Ar···I), but with structural relaxation of the Ag–I subunit at each value of r(Ar···I). D_e is the difference in energy between the potential energy minimum and the energy of the products Ar and Ag–I, the last at its ground-state equilibrium geometry.

For very weakly-bound complexes (such as Ar···H−X, where X is a halogen atom) it is a good approximation to assume that H−X is both rigid and of unperturbed geometry when in the complex. Novick [32] showed that for such complexes in the quadratic approximation, the intermolecular force constant $F_{22} = F_{\mathrm{Ar\cdots H}}$ (see below for the change of nomenclature) can be related to the equilibrium centrifugal distortion constant D_J^e of the complex and the equilibrium rotational constants $B_{\mathrm{e}}^{\mathrm{HX}}$ and $B_{\mathrm{e}}^{\mathrm{B\cdots HX}}$ of H−X and B···H−X, respectively, according to

$$D_J^{\mathrm{e}} = 16\pi^2\mu(B_{\mathrm{e}}^{\mathrm{B\cdots HX}})^3(1 - B_{\mathrm{e}}^{\mathrm{B\cdots HX}}/B_{\mathrm{e}}^{\mathrm{HX}})/\,F_{22} \qquad (3)$$

In the absence of equilibrium spectroscopic constants, ground state values are normally used in their place. In the limit that H−X can be treated as a point mass, eq.(3) reduces to the familiar expression for a diatomic molecule [33]:

$$D_J^{\mathrm{e}} = 16\pi^2\mu(B_{\mathrm{e}}^{\mathrm{B\cdots HX}})^3/\,F_{22} \qquad (4)$$

Millen [34] later generalized eq.(3) to include several types of weak hydrogen-bonded complex more complicated than linear triatomic molecules.

When the intermolecular bond in complexes of Lewis bases B with coinage metal halides M–X is strong, the approximation that the M–X force constant $F_{\mathrm{M–X}}$ is very much greater than $F_{\mathrm{B\cdots M}}$ (*i.e.* that M–X is rigid) is no longer a reasonable approximation. We have recently proposed [35] for such situations a more suitable model in which the centrifugal distortion constant D_J^{e} is expressed in terms of three quadratic force constants $F_{\mathrm{M–X}}$, $F_{\mathrm{B\cdots M}}$ (hereafter renamed as F_{11} and F_{22}, respectively) and the cross term F_{12}. In principle, this model allows the centrifugal distortion constants D_J^{e} of a sufficient number of isotopologues to be fitted to give F_{11}, F_{22} and F_{12}. In practice, because of ill-conditioning of the fit, it is necessary to assume that the cross term F_{12} is negligible and to fit the D_J^{e} values to give F_{22} at each of a range of fixed F_{11} values. The model applies to all complexes of Lewis bases B with any diatomic molecule (*e.g.* a hydrogen halide H−X, a dihalogen X−Y, or a coinage metal halide MX) as long as the diatomic molecule lies along a C_n ($n \geq 2$) symmetry axis of B in the equilibrium geometry.

For a linear triatomic molecule, such as Ar···Ag–I (with numbering of the Ag and I atoms and internal coordinates r_1 and r_2 as defined in Figure 2), the three force constant model leads, under the assumption $F_{12} = 0$, to the expression [35]

$$hD_J^e = \frac{1}{2}\left\{\frac{\hbar^4}{(I_{bb}^e)^4}\right\}\{(m_1 a_1)^2 (F^{-1})_{11} + (m_1 a_1 + m_2 a_2)^2 (F^{-1})_{22}\} \qquad (5),$$

where I_{bb}^e is the equilibrium principal moment of inertia of the complex and the a_n are equilibrium principal axis coordinates of atoms n = 1 and 2, and $(F^{-1})_{nn} = 1/F_{nn}$ under the approximations described. It was shown in ref. 35 that zero-point constants and coordinates can be used in place of equilibrium values as a reasonable approximation. When F_{22} is fitted by the least-squares method to the D_J^0 values of the two isopologues ^{40}Ar···^{107}Ag–^{127}I and ^{40}Ar··· ^{109}Ag–^{127}I for each of a series of assumed values of F_{11} and then F_{22} is plotted against F_{11}, the result is the curve shown in Figure 3. The equilibrium value of the force constant F_e = 145.8 N m^{-1} of the free diatomic molecule Ag–I can be obtained from the known equilibrium vibrational wavenumber [36] and is indicated in Figure 3. If it is assumed that F_{11} lies within the range ± 10% of the free Ag–I molecule value (reasonable in view of the weakness of the Ar···Ag bond established later), the result is F_{22} = 20.2(8) N m^{-1} for Ar···Ag–I.

It has been shown elsewhere [35] that if the M–X molecule can be assumed rigid ($F_{11} = \infty$ N m^{-1}) and unchanged in geometry when subsumed into the complex, eq.(5) reduces to eq.(3). It was also shown that eq.(3) and the corresponding versions due to Millen [34] will always underestimate F_{22}, although the extent of the underestimate is negligible for the weakly bound hydrogen-bonded complexes B···H–X, for which these equations were originally proposed. However, when F_{22} and F_{11} are of similar magnitude the underestimation becomes serious [31]. The diatomic (point mass) model, see eq.(4), overestimates F_{22}, on the other hand. We note that, when applied to Ar···Ag–I, eqs.(3) and (4) lead to F_{22} = 14.8 and 24.9 N m^{-1}, respectively, while the preferred value from eq.(5) is F_{22} = 20.2(8) N m^{-1}. Thus, even though the Ar atom in Ar···Ag–I is weakly bound compared with some B in other B ···M–X so far investigated [30,31], with F_{11} ~ 7F_{22}, eqs.(3) and (4) still under- and over-estimate F_{22} , respectively, albeit less seriously than in H_3P···Ag–I, for example [31].

The equilibrium dissociation energy D_e for the process Ar···Ag–I = Ar + Ag–I provides another measure of the strength of the interaction of Ar and Ag–I and was calculated at the CCSD(T)(F12*)/cc-pVTZ-F12 level of theory. The resulting value is $D_e = 16.7$ kJ mol^{-1} after counterpoise correction. The best available experimental measurement of the equilibrium dissociation energy for the process Ag–I = Ag + I is $D_e = 251$ kJ mol^{-1}, as calculated from $D_e = D_0 + \frac{1}{2}\omega_e - \frac{1}{4}\omega_e x_e$, where the zero-point dissociation energy D_0 = 250 kJ mol^{-1} is given in ref. [37] and the spectroscopic quantities ω_e and $\omega_e x_e$, are from ref. [36]. Thus, although by either measure of binding strength the Ar···Ag bond is about twice as strong as the hydrogen bond in a typical weak complex B···H–X ($F_{11} \approx 10$ N m^{-1}, $D_e \approx 10$ kJ mol^{-1}), it is still about an order of magnitude weaker than the Ag–I bond.

3.4 Electric charge redistribution on formation of Ar···Ag–I

The halogen nuclear quadrupole coupling constant $\chi_{aa}(\mathrm{X}) = eq_{aa}^{\mathrm{X}}Q^{\mathrm{X}}$ of a linear molecule Ar···Ag–X carries information about the electric charge distribution at X through the electric field gradient q_{aa}^{X} at the halogen nucleus along the molecular (a) axis direction. The ionicity i_c (or fractional ionic character) of the free Ag–X molecule is given, in the model due to Townes and Dailey [38], by

$$i_c = 1 + \frac{\chi_{aa}(\mathrm{X})}{eQ^{\mathrm{X}}q_{(n,1,0)}^{\mathrm{X}}} \qquad (6),$$

in which $q_{(n,1,0)}^{\mathrm{X}}$ is the contribution to the electric field gradient at X along the a-axis direction that arises from a single electron in np_a orbital. The quantities $eQ^{\mathrm{X}}q_{(n,1,0)}^{\mathrm{X}}$ are available (as frequencies) for X = Cl, Br and I from ref.[39]. Eq.(6) gives i_c= 0.570 for ^{40}Ar···^{107}Ag–^{127}I but has the value 0.537 for free ^{107}Ag–^{127}I, as indicated in Table 3, in which are collected values of several properties of Ag-I. This demonstrates that there is a small electric charge rearrangement within Ag–I on formation of the complex. The same approach applied to other B···Ag-I, where B is a Lewis base other than Ar, leads to somewhat larger increases in ionicity of Ag–I on complex formation [30,31].

4. Comparison of the properties of Ar···Ag–X for X = F, Cl, Br and I

All four molecules in the series Ar···Ag−X where X = F, Cl, Br and I have now been investigated by means of rotational spectroscopy (the spectroscopic data for X = F, Cl and Br are available from ref.[1]) and through *ab initio* calculations. It is timely to examine how the properties thereby determined vary with the halogen atom X. Table 2 sets out various properties of the Ar···Ag−X, as determined by the methods outlined for Ar···Ag−I in this article. The properties include: (a) the experimental bond distances r_0(Ar···Ag) and r_0(Ag–X), (b) the corresponding equilibrium distances r_e(Ar···Ag) and r_e(Ag–X) calculated at the CCSD(T)(F12c)/cc-pVTZ-F12 level, (c) the dissociation energy D_e for the process Ar···Ag−X = Ar + Ag−X calculated at the same level of theory (including corrections for basis set superposition error, which are very small for such explicitly correlated calculations), (d) the stretching force constants F_{22} for the Ar···Ag bond determined by fitting centrifugal distortion constants D_J^0 of available isotopologues using eq.(5) under the assumption that F_{11} for the Ag–X bond lies within 10 % of that of free Ag–X (see earlier), and (e) the ionicity of Ag–X when within Ar···Ag−X (as calculated from the nuclear quadrupole coupling constants from [1] and this work). Also included in Table 2 are the distances $r_m^{(2)}$ obtained by fitting the data reported by Evans and Gerry [1] for Ar···Ag−Cl and Ar···Ag−Br using the program STRFIT of Kisiel [29]. Although $r_m^{(2)}$ bond lengths are generally viewed as the best approximation to r_e values for polyatomic molecules, we note that they are not very well determined for these two molecules. Insufficient isotopic data are available for Ar···Ag−F and Ar···Ag−I to generate $r_m^{(2)}$ distances for these molecules.

For the purposes of comparing the properties of the Ar···Ag−X, it is convenient to collect together in Table 3 the set of corresponding quantities for the free Ag–X molecules, namely (a) values of the equilibrium Ag–X bond distances r_e as calculated from equilibrium rotational constants, (b) the equilibrium quadratic Ag–X stretching force constants F_e(Ag–X) as calculated from equilibrium centrifugal distortion constants D_J^e using eq.(4), (c) the most up-to-date values of the equilibrium dissociation energy D_e, as calculated from the zero-point experimental D_0 values [37] and ω_e and $\omega_e x_e$ values [36] by the method indicated in Section 3.3, and (d) the Ag–X

ionicities calculated from the published nuclear quadrupole coupling constants of Ag–Cl [40], Ag–Br [41] and Ag–I [42].

Several general trends in the properties of the series of molecules Ar···Ag−X (X = F, Cl, Br or I) may be discerned from Table 2. First, it is noted that, while the distance r(Ag–X) decreases significantly along the series X = I > Br > Cl > F, the distance r(Ar···Ag) varies by only about 0.1 Å. Secondly, the *ab initio* calculations establish unambiguously that each Ar···Ag−X molecule is linear at equilibrium, with good agreement between the calculated r_e bond lengths and the r_0 experimental values. Thirdly, Table 2 also reveals that the energy D_e required for the dissociation Ar···Ag−X = Ar + Ag−X has the order X = F > Cl > Br > I and increases in steps of 1-2 kJ mol^{-1}. Figure 4 shows how the intermolecular quadratic force constant $F_{22} = F_{\mathrm{Ar\cdots Ag}}$ (obtained by fitting centrifugal distortion constants D_J^0) varies with assumed values of the force constant $F_{11} = F_{\mathrm{Ag–X}}$ in the range 100-300 N m^{-1} for each of the four members of the Ar···Ag−X series. The variation of F_{22} over this range of F_{22} is smallest in the case of X = F, increases steadily through X = Cl and X = Br, and is largest for X = I. We note from Table 3 that the strength of the free Ag–X molecule, whether judged by the force constant F_e criterion or the dissociation energy D_e criterion, is in the order I < Br < Cl < F. Also shown in Figure 4 are the values of F_{22} obtained when the Ag–X subunit is taken as rigid, that is when F_{11} is assumed infinite. These values are identical to those that result from the use of eq.(3) and underline the fact that eq.(3) always underestimates F_{22}, with the underestimate increasingly more serious as the Ag–X bond weakens.

A consideration of the ionicity i_c of the series of complexes Ar···Ag−X in Table 2 and of the free molecule series Ag–X in Table 3 is of interest. The ionic character of Ag–X increases from I to Br to Cl (see Table 3) and this increases further by 6.1 %, 4.1 % and 2.7 %, respectively, when Ag–X enters into the complex Ar···Ag−X.

Finally, we note that a linear relationship exists between the two measures (D_e and F_{22}) of the strength of binding in the series of molecules Ar···Ag−X, where X = I, Br, Cl and I. Figure 5 shows that the plot of F_{22} versus D_e is a reasonable approximation to a straight line. The error bars are those implied by the assumption that F_{11} lies within ±10 % of the value F_e of the free Ag–X force constant when determining F_{22} from the plots in Figure 4. Similar linear relationships have

been noted previously [43] for hydrogen-bonded complexes B···H−X and halogen-bonded complexes B···X−Y for a wide range of Lewis bases, hydrogen halides H−X and dihalogens X−Y. Indeed, for all of the complexes B···HX and B···XY examined in [43], a single linear equation $F_{22} = mD_e$, having the same slope m = 6.8(1) x 10^{-4} mol m^{-2} within experimental error, was established. The slope of the line in the case of the series Ar···Ag−X is 1.8(2) x 10^{-3} mol m^{-2}, which is significantly different from that of the hydrogen- and halogen-bonded complexes and probably reflects a difference in binding.

5. Conclusions

Ar···Ag−I has been formed in the gas phase by laser ablation of a silver iodide rod in the presence of a pulse of argon gas and has been characterised both by rotational spectroscopy and by *ab initio* calculations at the CCSD(T)(F12c)/cc-pVTZ, explicitly correlated level of theory. The molecule has been shown to be linear in the ground state, with atoms in the order shown. The Ar···Ag and Ag–I bond lengths, the dissociation energy D_e for the process Ar···Ag−I = Ar + Ag−I, the intermolecular quadratic stretching force constant $F_{Ar\cdots Ag} = F_{22}$ and the change in the ionicity i_c of Ag–I when it enters the complex have been presented. The opportunity has been taken to compare the way in which these properties vary along the series Ar···Ag−X (X = F, Cl, Br and I).

6. Acknowledgements.

The authors thank the European Research Council for the postdoctoral fellowship awarded to C.M., a PhD studentship awarded to J.C.M, and for project funding (Grant No. CPFTMW-307000). A.C.L. thanks the University of Bristol for a Senior Research Fellowship and Newcastle University for a Visiting Professor award. We are grateful to Dr Grant Hill of the University of Sheffield for generous help in providing, and setting up, Ag basis functions to be used in *ab initio* calculations at the CCSD(T)(F12c) level of theory.

References.

[1] C.J. Evans and M.C.L. Gerry, J. Chem. Phys. 112 (2000) 1321-1329.

[2] T.J. Balle and W.H. Flygare, Rev. Sci. Instrum. 52 (1981) 33-45.

[3] S.J. Harris, S.E. Novick and W. Klemperer, J.Chem. Phys. 60 (1974) 3208-3209.

[4] S.E. Novick, P. Davies, S.J. Harris and W. Klemperer, J. Chem. Phys. 59 (1973) 2273-2279.

[5] M. R. Keenan, E.J. Campbell, T.J. Balle, L.W. Buxton, T.K. Minton, P.D. Soper and W.H. Flygare, J. Chem. Phys. 72 (1979) 3070-3080.

[6] A. McIntosh, Z. Wang, J. Castillo-Chará, R.R. Lucchese, J.W. Bevan, R.D. Suenram and A.C. Legon, *J. Chem. Phys.*, 111 (1999) 5764-5770.

[7] S.J. Harris, S.E. Novick, W. Klemperer and W.E.Falconer, J. Chem. Phys. 61 (1974) 193-197.

[8] Y. Xu, W. Jäger, I. Ozier and M.C.L. Gerry, J. Chem. Phys. 93 (1993) 3726-3731.

[9] J.B. Davey, A.C. Legon and E.R. Waclawik, Chem. Phys. Lett. 346 (2001) 103-111.

[10] J.B. Davey, A.C. Legon, and E.R. Waclawik, Chem. Phys. Lett. 306, (1999) 133-144.

[11] S.L. Stephens, W. Mizukami, D.P. Tew, N.R. Walker and A.C. Legon, J. Chem. Phys. 136, (2012) 064306.

[12] S.L. Stephens, N.R. Walker, J. Mol. Spectrosc. 263 (2010) 27–33.

[13] D.P. Zaleski, S.L. Stephens and N.R. Walker, Phys. Chem. Chem. Phys. 16 (2014) 25221-25228.

[14] H.-J.Werner, P. J. Knowles, R. Lindh, F. R. Manby, M. Schutz et al., MOLPRO,version 2009.1, a package of ab initio programs, 2009, see http://www.molpro.net.

[15] C. Hättig, D.P. Tew and A. Köhn, J. Chem. Phys. 132 (2010) 231102.

[16] C. Hättig, W. Klopper, A. Köhn and D.P. Tew, Chem. Rev. 112 (2012) 4-74.

[17] K. Raghavachari, G. W. Trucks, J. A. Pople and M. A. Head-Gordon, Chem. Phys. Lett. 157 (1989) 479-483.

[18] S. F. Boys and F. Bernardi, Mol. Phys**.** 19 (1970) 553-566.

[19] G. Knizia and H.-J. Werner, J. Chem. Phys. 128 (2008) 154103.

[20] G. Knizia, T. B. Adler and H.-J. Werner, J. Chem. Phys. 130 (2009) 054104.

[21] J.G. Hill and K.A. Peterson, J. Chem. Phys. 141 (2014) 094106. See http://bit.ly/ccBasis for a repository of basis functions, including cc-pVTZ-F12 for Br and I, constructed by J.G. Hill.

[22] J.G. Hill and K.A. Peterson, J. Chem. Theory Comput., 8 (2012) 518-526.

[23] K.A. Peterson and C. Puzzarini, Theo. Chem. Acc., 114 (2005) 283-296.

[24] M. Dolg, U. Wedig, H. Stoll and H. Preuss, J. Chem. Phys., 86, (1987) 866-872.

[25] K.A. Peterson, D. Figgen, E. Goll, H. Stoll and M. Dolg, J. Chem. Phys. 119 (2003) 11113-11123.

[26] PGOPHER , a program for simulating rotational structure, designed by C. M. Western, University of Bristol ,version 6.0.202, 2010. Available at http://pgopher.chm.bris.ac.uk.

[27] C. C. Costain, J. Chem. Phys. 29 (1958) 864.

[28] C.C. Costain, Trans. Am. Crystallog.Assoc. 2 (1966) 157-164.

[29] Z. Kisiel, J. Mol. Spectrosc. 218 (2003) 58-67.

[30] D. M. Bittner, S. L. Stephens, D. P. Zaleski, D. P. Tew, N. R. Walker and A. C. Legon, Phys. Chem. Chem. Phys. 18 (2016) 13638-13645.

[31] S. L. Stephens, D. P. Tew, N. R. Walker and A. C. Legon, Phys. Chem. Chem. Phys. 18 (2016) 18971-18977.

[32] S. E. Novick, J. Mol. Spectrosc. 68 (1977) 77-80.

[33] Molecular Spectra and Molecular Structure, Vol. I. Spectra of Diatomic Molecules, G. Herzberg, Second Edition, Van Nostrand Reinhold Co., New York, 1950, p103

[34] D.J. Millen, *Can. J. Chem*. 63 (1985) 1477-1479.

[35] D.M. Bittner, N.R. Walker and A.C. Legon, J. Chem. Phys.144 (2016) 074308.

[36] F.J. Lovas, E. Tiemann, J.S. Coursey, S.A. Kotochigova, J. Chang, K Olsen, and R. A. Dragoset, NIST Diatomic Spectral Database (created 12September 2009; updated 12 December 2014), http://www.nist.gov/pml/data/msd-di/

[37] D.L. Hildenbrand and K.H. Lau, J. Phys. Chem. A 110 (2006) 11886-11889.

[38] C. H. Townes and B. P. Dailey, *J. Chem. Phys.*, **23**, 118 (1955).

[39] W. Gordy, R.L. Cook, *Microwave Molecular Spectra*, in:A. Weissberger (Ed.), Techniques of Chemistry, Wiley, New York, 1984. Chapter XIV, Table 14.5, p 752.

[40] C. Styger and M.C.L Gerry, Chem. Phys. Lett. 188 (1992) 213-216.

[41] J. Hoeft, F.J. Lovas, E. Tiemann and T. Törring, Z. Naturforsch. A 26 (1971) 240-244.

[42] S.G Batten, A.G. Ward and A.C. Legon, J. Mol. Struct**.** 780-781 (2006) 300-305.

[43] A.C. Legon, Phys. Chem. Chem. Phys. 16 (2014) 12415-12421. See correction: Phys. Chem. Chem. Phys 16 (2014) 25199.

Tables

Table 1

Observed spectroscopic constants[a] of ^{40}Ar··· ^{107}Ag–^{127}I and ^{40}Ar··· ^{109}Ag–^{127}I

Spectroscopic constant	^{40}Ar···^{107}Ag–^{127}I	^{40}Ar··· ^{109}Ag–^{127}I
B_0/MHz	541.42280(10)	540.71464(10)
D_J/kHz	0.05773(24)	0.05686(23)
$\chi_{aa}(\mathrm{I})/\mathrm{MHz}$	-985.411(54)	-985.30(14)
σ_{RMS}/kHz[b]	7.1	6.7
N[c]	68	66

[a] Numbers in parentheses are one standard deviation in units of the last significant digits.

[b]Root-mean square deviation of the fit.

[c]Number of nuclear quadrupole hyperfine components included in fit.

Table 2

Properties of the series Ar···Ag–X available either experimentally[a] or calculated *ab initio* at the CCSD(T)(F12c)/cc-pVTZ-F12 level of theory

Property	Ar···Ag–F	Ar···Ag–Cl	Ar···Ag–Br	Ar···Ag–I
r_0(Ar···Ag)/Å	2.5581[b]	2.6124(4)[c]	2.6366(6)[c]	2.6759[b]
r_0(Ag–X)/Å	1.9861[b]	2.2683(4)[c]	2.3825(4)[c]	2.5356[b]
∠ArAgX^{calc} / º	179.82	180.00	180.06	180.04
r_e^{calc}(Ar···Ag)/Å	2.5748	2.6150	2.6385	2.6713
r_e^{calc}(Ag···X)/Å	1.9743	2.2759	2.3927	2.5507
$r_m^{(2)}$(Ar···Ag)/Å	…	2.610(7)[d]	2.640(10)[d]	…
$r_m^{(2)}$(Ag···X)/Å	…	2.2673(4)[d]	2.3821(6)[d]	…
$F_{22}/(\mathrm{N\ m^{-1}})$ [e]	29.3(2)	25.8(2)	23.5(6)	20.2(8)
$D_e^{calc}/(\mathrm{kJ\ mol^{-1}})$ [f]	21.8	19.3	18.0	16.7
Ionicity, i_c [g]	…	0.686	0.638	0.570

[a]Numbers in parentheses are one standard deviation in units of the last significant figure.

[b] These r_0 bond lengths result from an exact fit to the ground-state rotational constants of two isotopologues (this work or ref. [1]) and therefore no errors are available.

[c]These r_0 bond lengths result from a fit of ground-state rotational constants of all isotopologues of the appropriate Ar···Ag–X reported in ref. [1].

[d] $r_m^{(2)}$values fitted to rotational constants of all isotopologues reported in ref. [1].

[e]Calculated by a least-squares fit of D_J^0values of all available isotopologues to eq.(5) by assuming F_{11} is the experimental value of the free molecule AgX (see Table 3) and $F_{12} = 0$. The error is that generated if F_{11} for Ar···Ag–X lies within the range ± 10% of that of free AgX.

[f]Values calculated at the CCSD(T)(F12c)/cc-pVTZ-F12 level of theory, corrected for basis set superposition error. See Section 2 for definition of basis functions used.

[g] See eq.(6) for definition.

Table 3.

Experimental properties[a] of Ag–X (X = F, Cl, Br or I) and those calculated at the CCSD(T)(F12c)/cc-pVTZ-F12 level of theory

Property	Ag–F	Ag–Cl	Ag–Br	Ag–I
r_e^{exp}/Å[b]	1.98318	2.28079	2.39311	2.54462
r_e^{calc}/Å	1.9872	2.2867	2.4020	2.5575
$(r_e^{exp} - r_e^{calc})$/Å	-0.0040	-0.0059	-0.0089	-0.0129
F_e^{exp}/(N m^{-1})[c]	251.6	183.2	166.6	145.8
F_e^{calc}/(N m^{-1})[d]	248.4	178.3	161.9	142.9
$(F_e^{exp} - F_e^{calc}/)$(N m^{-1})	3.1	4.9	4.7	2.9
$D_e^{exp}/$(kJ mol^{-1})[e]	344	313	280	251
Ionicity, i_c [f]	‘’’	0.668	0.613	0.537

[a] r_e, F_e and D_e are the equilibrium values of the internuclear distance, quadratic force constant and dissociation energy, respectively.

[b] Value calculated from equilibrium rotational constant B_e of the most abundant isotopologue (see ref. [36] for equilibrium spectroscopic constants).

[c] Value calculated from the equilibrium centrifugal distortion constant D_J^e of the most abundant isotopologue (see ref. [36] for equilibrium spectroscopic constants).

[d] Calculated at the CCSD(T)(F12c)/ccpVTZ-F12 level of theory. See Section 2.2 for definition of the basis functions employed.

[e] Calculated from the experimental D_0 values reported in ref. [37] by means of $D_e = D_0 + \frac{1}{2}\omega_e - \frac{1}{4}\omega_e x_e$, with ω_e and $\omega_e x_e$ taken from ref. [36].

[f] See eq.(6) for definition.

Figures and Captions

Figure 1

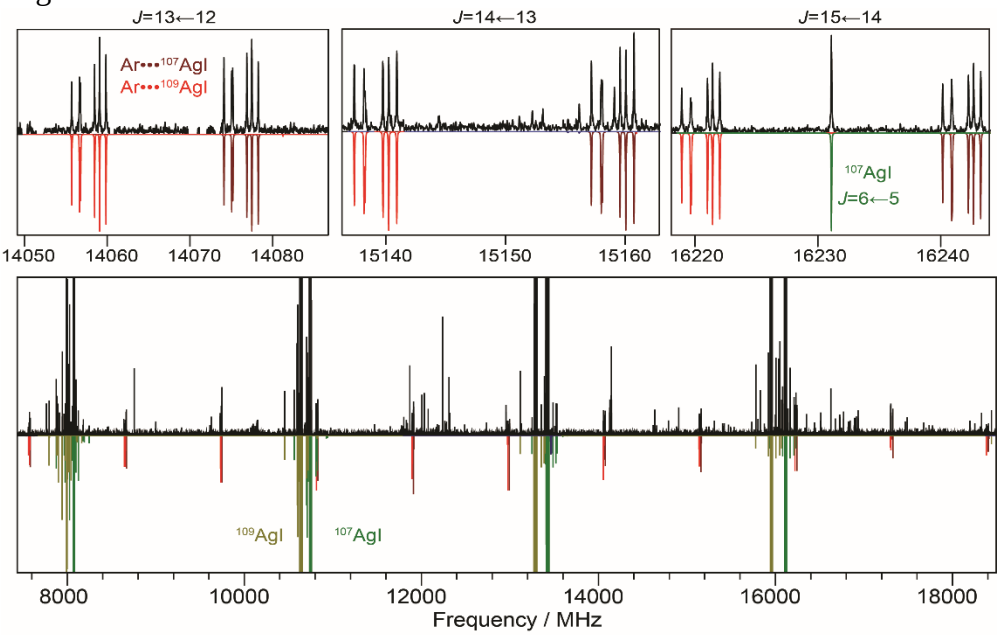

Bottom panel: Broadband spectrum recorded while probing a sample containing AgI and Ar (485k FIDs). Other molecules, apart from Ar···Ag–I, are present in the spectrum and of these only Ag–I is indicated. The downward pointing spectra have been simulated by means of known spectroscopic constants and are colour coded as follows: transitions of ^{107}AgI and ^{109}AgI are green and silver, respectively; red, downward pointing transitions are those synthesized by using the spectroscopic constants determined here (see Table 1) for Ar···^{107}AgI and Ar···^{109}AgI

Top three panels: Expanded parts of the spectrum in the regions of the J=13←12, 14←13 and 15←14 transitions of Ar···^{107}Ag–I (darker red in the simulation)) and Ar···^{109}Ag–I (lighter red in the simulation).

Figure 2

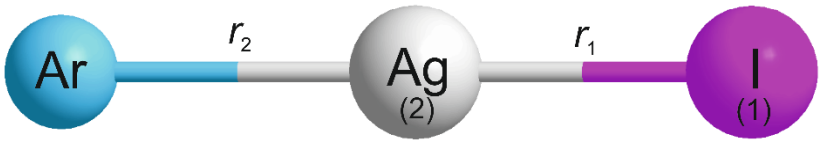

The molecular geometry of Ar···AgI drawn to scale. The internal coordinates r_1 and r_2 used in the discussion of how to obtain force constant F_{22} from the centrifugal distortion constants D_J^0 are indicated. The experimental zero-point values of r_1 and r_2 are r_0(Ag−I) = 2.5356 Å and r_0(Ar···Ag) = 2.6759 Å, respectively.

Figure 3

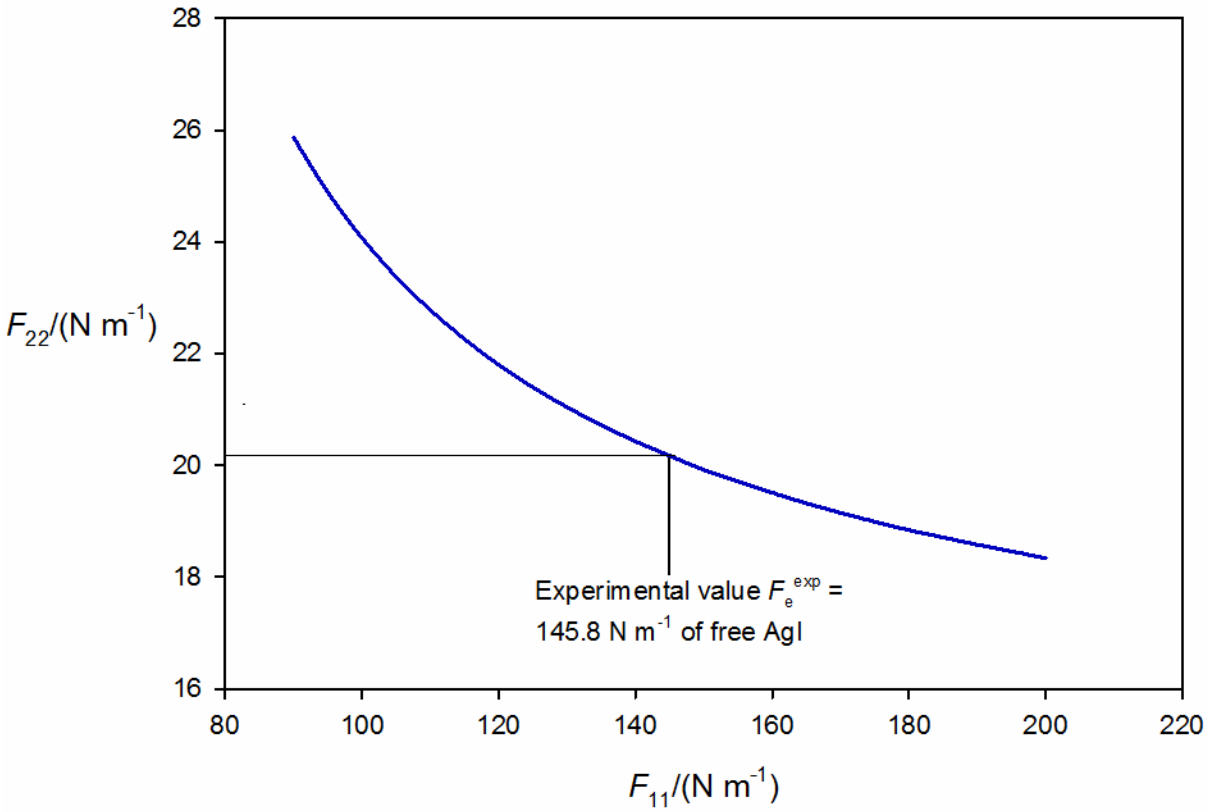

Values of the quadratic intermolecular stretching force constant F_{22} obtained by fitting the centrifugal distortion constants D_J^0 of the isotopologues ^{40}Ar$\cdots$ ^{107}Ag–^{127}I and ^{40}Ar$\cdots$ ^{109}Ag–^{127}I with eq.(5) at fixed values of the Ag–I stretching force constant F_{11} in the range 90 to 200 N m^{-1}. Eq.(5) is valid only if $F_{12} = 0$ is assumed for the off-diagonal force constant. The experimental equilibrium value F_e^{exp} of the free AgI molecule and the F_{22} value implied if it is assumed that $F_{11} = F_e^{exp}$ are indicated.

Figure 4

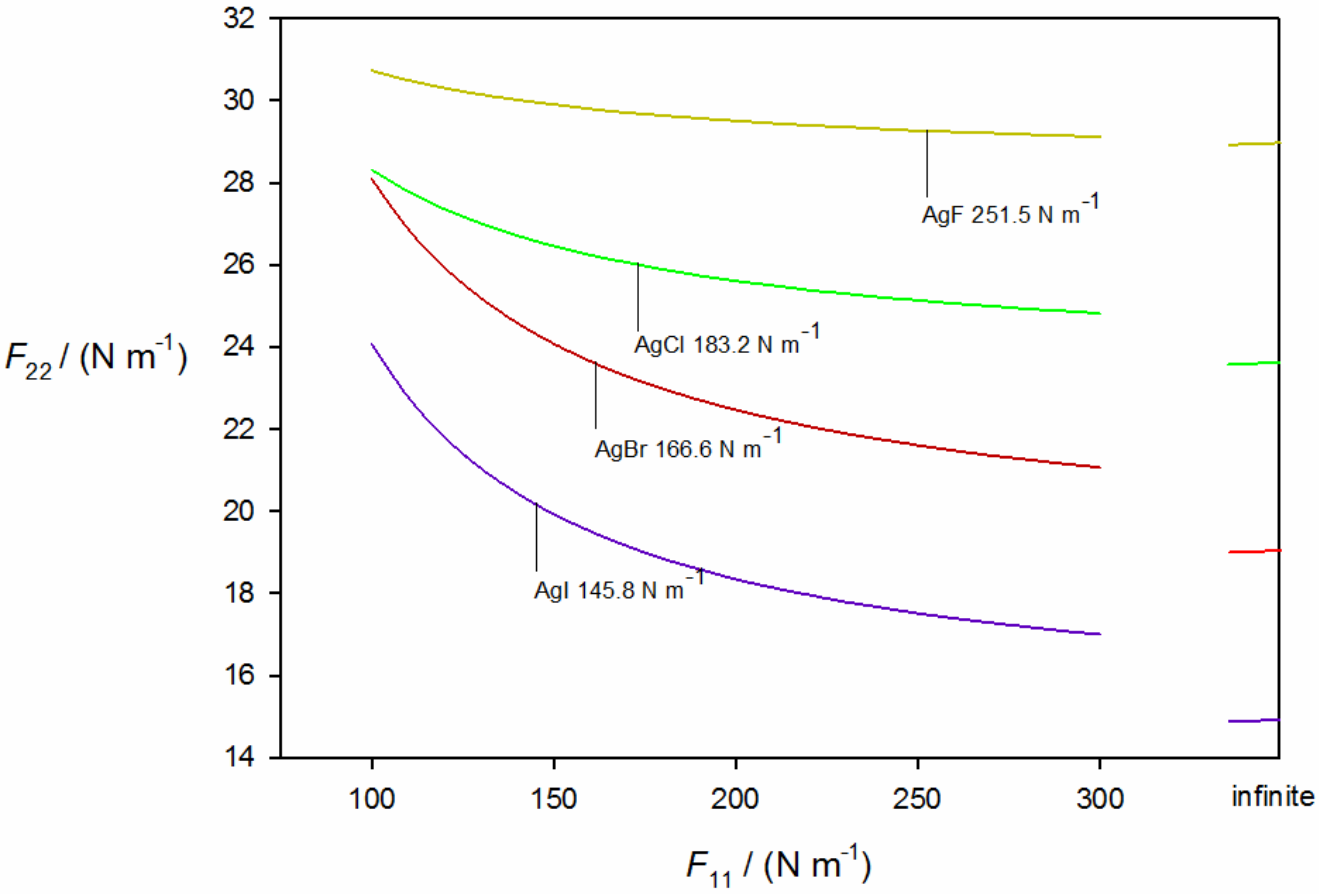

Values of the quadratic intermolecular stretching force constants F_{22} obtained by fitting the centrifugal distortion constants D_J^0 of all the available isotopologues of each member of the Ar···Ag–X series (X= F, Cl, Br and I) using eq.(5) at fixed values of the Ag–X stretching force constant F_{11} in the range 100 to 300 N m^{-1}. Eq.(5) is valid only if $F_{12} = 0$ is assumed for the off-diagonal force constant. The experimental equilibrium values of F_e^{exp} for the free Ag–X molecules (see Table 3) and the F_{22} values implied if it is assumed that $F_{11} = F_e^{exp}$ are indicated. At the extreme right-hand side of the graphs are shown the values to which F_{22} tends in the limit of infinite F_{11}, that is when the Ag–X is assumed rigid.

Figure 5

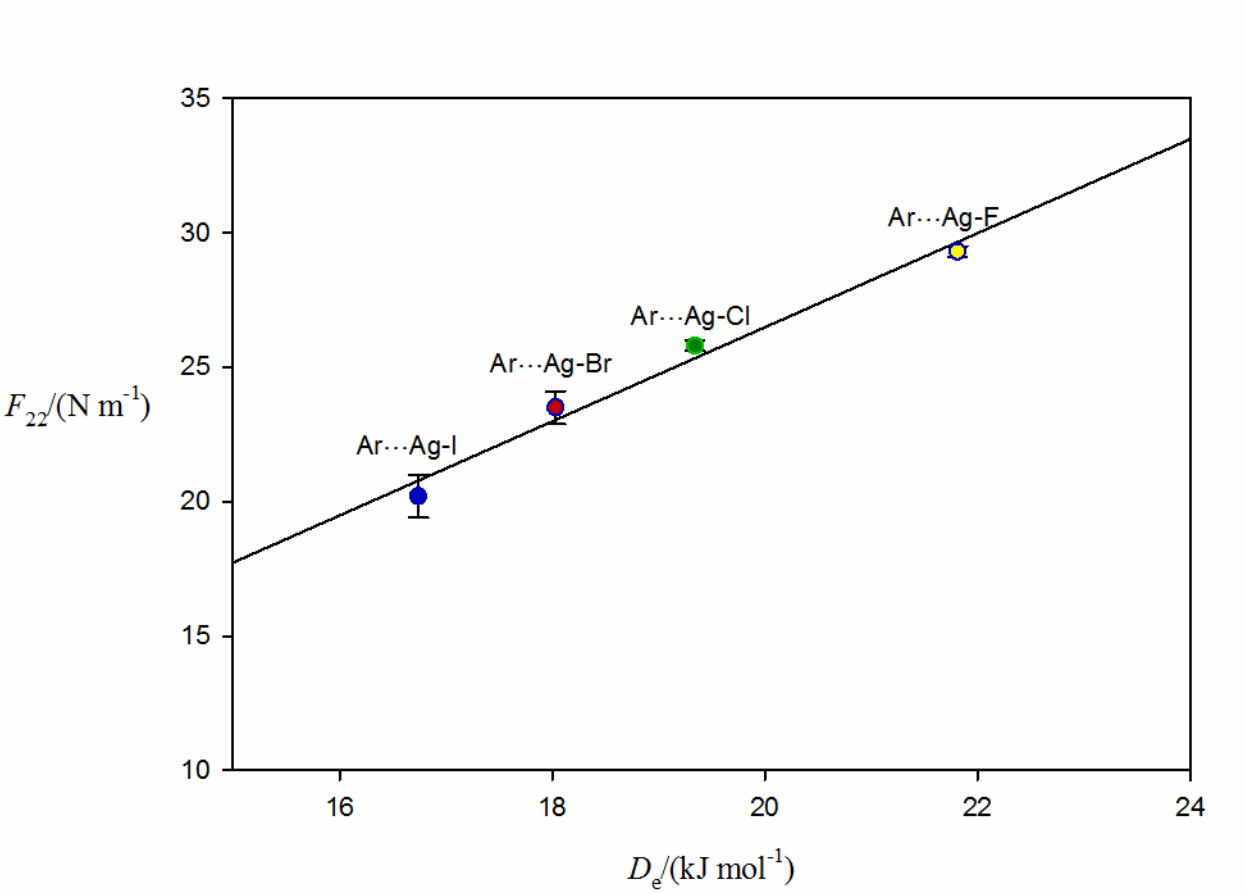

The variation of the Ar···Ag intermolecular quadratic stretching force constant F_{22} of Ar···Ag–X with the *ab initio* calculated equilibrium dissociation energy D_e for the process Ar···Ag–X = Ar + Ag–X, for X = F, Cl, Br and I. See text for the method of evaluation of the F_{22} and for the origin of the D_e values. The error bars indicate the range in F_{22} that results when F_{11} is assumed to lie within ±10% of the equilibrium force constant F_e^{exp} of the free Ag–X molecule (see Figure 4).